Polymer 51 (2010) 702–708

Contents lists available at ScienceDirect

Polymer

journal homepage: www.elsevier.com/locate/polymer

The vesicle formation in a binary amphiphilic diblock copolymer/homopolymer solution

Yuejin Zhu*, Qinghua Yang, Chaohui Tong, Ming Li, Xian Yu

Department of Physics, Ningbo University, 818 Fenghua Road, Ningbo 315211, China

ARTICLE INFO

Article history:
Received 12 March 2009
Received in revised form
1 June 2009
Accepted 7 July 2009
Available online 22 July 2009

Keywords:
Diblock copolymer
Homopolymer
Vesicles

ABSTRACT

The formation of vesicles in a binary blend of an amphiphilic diblock copolymer *AB*/homopolymer *C* was studied in a dilute solution using the real space two-dimensional self-consistent field theory (SCFT). Special attention was played to the role played by the homopolymer *C* in controlling the vesicle formation. In the simulations, it was found that as the averaged volume fraction of homopolymer *C* was decreased while keeping the total averaged volume fraction of block copolymer *AB* and homopolymer *C* unchanged, there was a morphological transition from the bilayer vesicles to rod-like/circle-like micelles. The compound vesicle structure was observed in the simulations. When the averaged volume fraction of block copolymer *AB* was further increased while the total averaged volume fraction of *AB* and *C* remained unchanged, the compound vesicle structure became less favored entropically than the unilamellar vesicle structure. The effect of the degree of polymerization of the homopolymer *C* on the vesicle formation of the amphiphilic system was examined. By reducing the degree of polymerization of the homopolymer *C* to unity, the component *C* became a small solvent molecule immiscible with the bulk solvent. It was found that the small solvent *C* exerted no influence on the morphological stability of the vesicles.

1. Introduction

The self-assembly of amphiphilic block copolymers in solutions can give rise to a variety of microstructures [1–18]. Besides the spherical and cylindrical micelles and bilayer vesicles, many other exotic morphologies have been observed in experiments, such as onion vesicles, genus vesicles, toroidal micelles with one or several rings, net or cage micelles [2–15]. From a thermodynamic point of view, the microstructures of amphiphilic block copolymers in solutions are determined by the delicate balance among the three competing interactions, i.e., the chain stretching in the core, the interfacial tension and the repulsion among corona chains [2]. Furthermore, kinetic factors such as the diffusion ability of the amphiphilic molecules and the details of the preparation procedures also come into play in determining the morphologies of the amphiphilic systems [19,20]. Among the various morphologies formed in the amphiphilic systems, the vesicle formation is of fundamental and practical importance, because it has many potential applications in areas such as micro-reactors, microcapsules, and drug delivery systems.

Due to its importance, a wide variety of theoretical approaches, including coarse-grained surface models [21–23], Monte-Carlo simulations [24,25], Brownian dynamic simulations [26,27], dynamic density functional theory (DDFT) [28], and dissipative particle dynamics [29] have been employed to investigate the vesicle formation. He et al. investigated the dynamics of the spontaneous formation of vesicle and toroidal micelles in amphiphilic block copolymer systems by employing the external potential dynamics (EPD) method, which is equivalent to dynamical SCFT with a nonlocal dynamics [19,20]. In their studies, a new pathway of spontaneous vesicle formation was discovered, in which the micelles do not coalesce, but simply grow by attracting copolymers from the solution, forming bigger micelles with a hydrophilic core. Finally, solvent molecules diffuse into the core, resulting in full vesicles. Recently, real-space self-consistent field theory (SCFT) has emerged as an attractive computational tool for the study of the vesicle formation [30–33]. Liang and coworkers performed two-dimensional (2D) real-space SCFT study of the formation of complex micelles including vesicles [30]. By tailoring the various interaction parameters and the initial fluctuation, different morphologies were observed. Using SCFT in 2D, Jiang et al. examined the effect of polydispersity on the vesicle formation in amphiphilic block copolymer systems [31]. It was found that larger polydispersity favors the formation of smaller vesicles or quasi-vesicles. This effect can be attributed to the segregation of copolymers according to their chain lengths. Wang, et al. studied the aggregate morphologies of amphiphilic *ABC* triblock copolymer consisting of one hydrophilic end block A and two hydrophobic blocks *B* and *C* in

* Corresponding author.
E-mail address: zhuyuejin@nbu.edu.cn (Y. Zhu).

0032-3861/$ – see front matter Crown Copyright © 2009 Published by Elsevier Ltd. All rights reserved.
doi:10.1016/j.polymer.2009.07.027

a dilute solution using SCFT in 2D [32]. Compared to the diblock copolymer systems, more complicated morphologies were observed in this triblock copolymer system. It was found that the transition from vesicles to circle-like micelles takes place with increasing the hydrophobicity of the *B* and *AB* blocks.

So far, the theoretical and computational studies of the vesicle formation are restricted to single-component amphiphilic block copolymer systems. On the contrary, there are many experimental studies on the vesicle formation in binary amphiphilic block copolymer/homopolymer systems [34–44]. Gao et al. reported a controllable vesicle formation of a diblock copolymer of poly(ethyleneoxide)-block-polybutadiene(PEO-b-PB) and a homopolymer of poly(acrylic acid) (PAA) in a solvent mixture of THF and *n*-dodecane [40]. The assembly was driven by the hydrogen-bonding complexation between the complementary binding sites on PEO and PAA. The very interesting finding in their study was that the vesicles can load PAA far above the stoichiometrical monomer ratio of PAA to PEO ([AA]/[EO]). At [AA]/[EO] in between 0.8 and 2.5, unilamellar vesicles with a constant membrane thickness were obtained. Further increasing [AA]/[EO] above 3 led to the formation of multivesicular vesicled (MVVs) in which many smaller vesicles resided. Motivated by Gao's interesting findings in the PEO-b-PB/PAA binary amphiphilic system, we performed a real-space 2D SCFT study of the vesicle formation in a generic binary amphiphilic block copolymer/homopolymer system, where the homopolymer is hydrophobic. The rest of the paper is organized as follows. In section II, the self-consistent field theory (SCFT) for the binary amphiphilic block copolymer/homopolymer system is briefly outlined and the governing equations are presented. In section III, results concerning the morphologies and vesicle formation of the binary block copolymer/homopolymer system are presented and discussed. Special attention is paid to the role played by the homopolymer on controlling the morphologies and vesicle formation. In section IV, the main conclusions of the present study are summarized.

2. Theory

We employ the self-consistent field theory to study the formation of micelles and vesicles in a solution consisting of n_p linear *AB* diblock copolymers and n_c linear *C* homopolymers with n_s solvent molecules. Each copolymer chain consists of *N* segments with a fixed monomer volume $1/\rho_0$, each homopolymer chain consists of αN segments with the same volume $1/\rho_0$, and each solvent molecule occupies the same volume $v_s = 1/\rho_0$. Therefore, the total volume of the system is $V = n_p N/\rho_0 + n_c \alpha N/\rho_0 + n_s/\rho_0$, and the system is assumed to be incompressible. Furthermore, we assume that the *A*, *B*, and *C* segments have the same segment length *a*. The fraction of A-monomer in a copolymer chain is denoted by *f*. The average volume fractions of copolymers, homopolymers, and solvent molecules are $\overline{\varphi}_{AB}$, $\overline{\varphi}_C$, and $\overline{\varphi}_S$, respectively. $w_A(\vec{r})$, $w_B(\vec{r})$, $w_C(\vec{r})$, $w_S(\vec{r})$ are the conjugate fields to the local volume fractions $\varphi_A(\vec{r})$, $\varphi_B(\vec{r})$, $\varphi_C(\vec{r})$, $\varphi_S(\vec{r})$ respectively in a space point $\vec{r}$. The dimensionless free energy of the system is given by

$$\begin{aligned}\frac{NF}{\rho_0 K_B T V} = & -\overline{\varphi}_{AB}\ln\left(\frac{Q_{AB}}{V\overline{\varphi}_{AB}}\right) - \frac{\overline{\varphi}_C}{\alpha}\ln\left(\frac{Q_C}{V\overline{\varphi}_C}\right) - \overline{\varphi}_S N \ln\left(\frac{Q_S}{V\overline{\varphi}_S}\right) \\ & + \frac{1}{V}\int \mathrm{d}\vec{r}\Big[\chi_{AB}N\varphi_A(\vec{r})\varphi_B(\vec{r}) + \chi_{AC}N\varphi_A(\vec{r})\varphi_C(\vec{r}) + \chi_{AS}N\varphi_A(\vec{r})\varphi_S(\vec{r}) \\ & + \chi_{BC}N\varphi_B(\vec{r})\varphi_C(\vec{r}) + \chi_{BS}N\varphi_B(\vec{r})\varphi_S(\vec{r}) + \chi_{CS}N\varphi_C(\vec{r})\varphi_S(\vec{r}) \\ & - w_A(\vec{r})\varphi_A(\vec{r}) - w_B(\vec{r})\varphi_B(\vec{r}) - w_C(\vec{r})\varphi_C(\vec{r}) - w_S(\vec{r})\varphi_S(\vec{r}) \\ & - \xi(\vec{r})(1 - \varphi_A(\vec{r}) - \varphi_B(\vec{r}) - \varphi_C(\vec{r}) - \varphi_S(\vec{r}))\Big] \end{aligned} \tag{1}$$

where k_B is the Boltzmann constant and *T* is the absolute temperature, and χ_{ij} is the Flory–Huggins interaction parameter between species *i*, *j*. $\xi(\vec{r})$ is the Lagrange multiplier which enforces the incompressibility condition of the system. Q_{AB} is the partition function of one copolymer chain, Q_C is the partition function of one homopolymer chain, and Q_S is the partition function of the solvent, and they have the following expressions:

$$Q_{AB} = \int \mathrm{d}\vec{r} q_1(\vec{r},s) q_1^+(\vec{r},s) \tag{2}$$

$$Q_C = \int \mathrm{d}\vec{r} q_2(\vec{r},s) q_2(\vec{r},1-s) \tag{3}$$

$$Q_S = \int \mathrm{d}\vec{r} \exp(-w_s(\vec{r})/N) \tag{4}$$

where $q(\vec{r},s)$ represents the probability of finding a segment with contour length *s* at position $\vec{r}$, $q_1(\vec{r},s)$ and $q_1^+(\vec{r},s)$ satisfy the following modified diffusion equations

$$\frac{\partial q_1(\vec{r},s)}{\partial s} = \nabla^2 q_1(\vec{r},s) - w(\vec{r}) q_1(\vec{r},s) \tag{5}$$

$$\frac{\partial q_1^+(\vec{r},s)}{\partial s} = -\nabla^2 q_1^+(\vec{r},s) + w(\vec{r}) q_1^+(\vec{r},s) \tag{6}$$

where $w = w_A$ when $0 < s < f$, and w_B when $f < s < 1$, with the initial conditions of $q_1(\vec{r},0) = 1$, and $q_1^+(\vec{r},1) = 1$, respectively. However the homopolymer only requires one segment distribution function $q_2(\vec{r},s)$, which satisfies

$$\frac{\partial q_2(\vec{r},s)}{\partial s} = \nabla^2 q_2(\vec{r},s) - w(\vec{r}) q_2(\vec{r},s) \tag{7}$$

where $w = w_C$ when $0 < s < \alpha$, with the initial condition of $q_2(\vec{r},0) = 1$.

Minimizing the free energy in Eq. (1) with respect to the local volume fractions and their conjugate fields as well as the Lagrange multiplier, the following self-consistent equations describing the equilibrium morphologies of the system can be obtained

$$\varphi_A(\vec{r}) = \frac{\overline{\varphi}_{AB} V}{Q_{AB}} \int_0^f \mathrm{d}s q_1(\vec{r},s) q_1^+(\vec{r},s) \tag{8}$$

$$\varphi_B(\vec{r}) = \frac{\overline{\varphi}_{AB} V}{Q_{AB}} \int_f^1 \mathrm{d}s q_1(\vec{r},s) q_1^+(\vec{r},s) \tag{9}$$

$$\varphi_C(\vec{r}) = \frac{\overline{\varphi}_C V}{Q_C \alpha} \int_0^\alpha \mathrm{d}s q_2(\vec{r},s) q_2(\vec{r},\alpha - s) \tag{10}$$

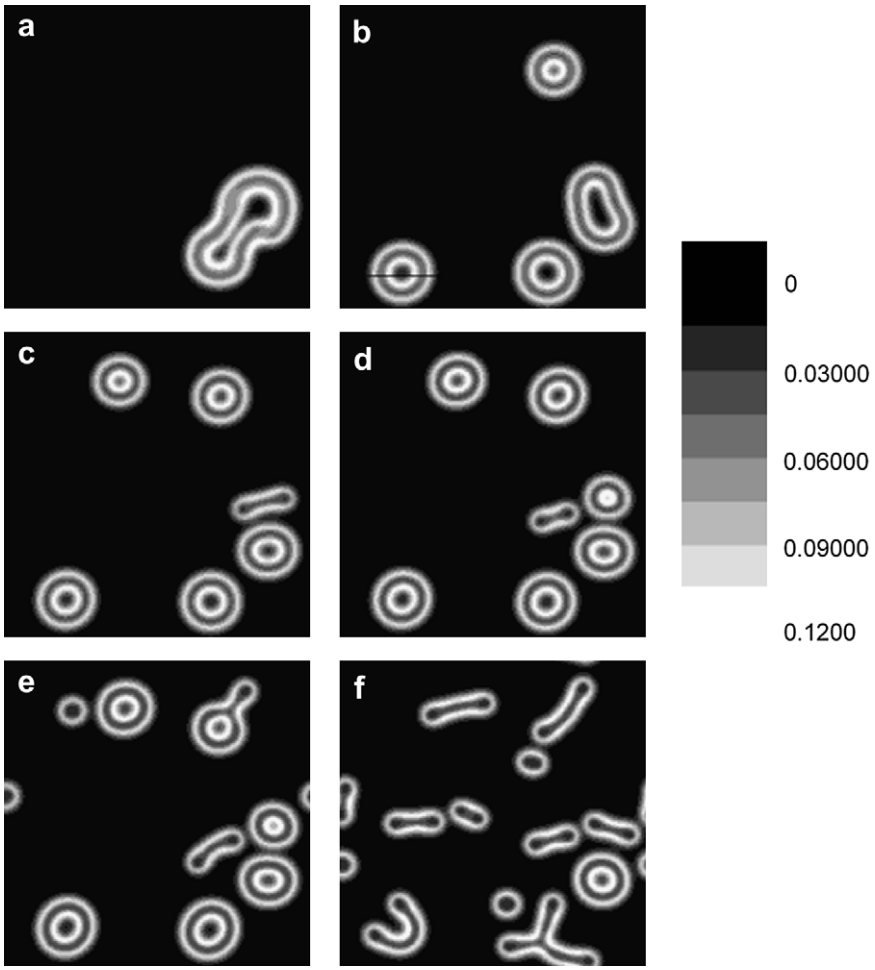

Fig. 1. Density distributions of diblock *A* with copolymer *AB*, homopolymer *C*, and solvent *S*. Interaction parameters $\chi_{AS}N = 0.5$, $\chi_{BS}N = 30.0$, $\chi_{CS}N = 20.0$, $\chi_{BC}N = 0.0$, $\chi_{AB}N = \chi_{AC}N = 9.0$, with an increase in the copolymer concentration $\overline{\varphi}_{AB}$: (a) $\overline{\varphi}_{AB} = 0.04$, (b) $\overline{\varphi}_{AB} = 0.05$, (c) $\overline{\varphi}_{AB} = 0.06$, (d) $\overline{\varphi}_{AB} = 0.07$, (e) $\overline{\varphi}_{AB} = 0.08$, (f) $\overline{\varphi}_{AB} = 0.09$. White and dark regions correspond to high and low volume fractions of block *A*, respectively.

$$\varphi_S(\vec{r}) = \frac{\overline{\varphi}_S V}{Q_S}\exp(-W_S(\vec{r})/N) \tag{11}$$

$$w_A(\vec{r}) = \chi_{AB}N\varphi_B + \chi_{AC}N\varphi_C + \chi_{AS}N\varphi_S + \xi(\vec{r}) \tag{12}$$

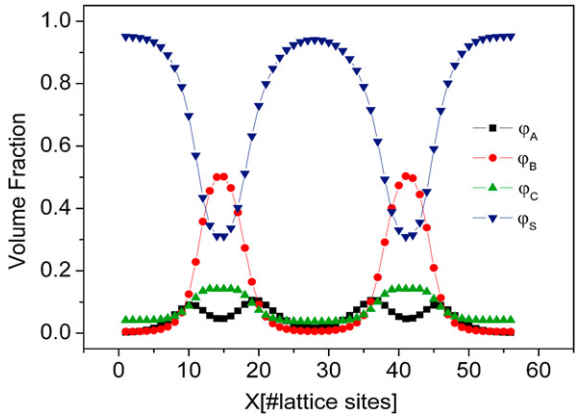

Fig. 2. (Color online) Density distributions of each constituent of the system along the intercepting line through the center of the vesicle are displayed, corresponding to Fig. 1 (b). (For interpretation of the references to color in this figure legend, the reader is referred to the web version of this article.)

$$w_B(\vec{r}) = \chi_{AB}N\varphi_A + \chi_{BC}N\varphi_C + \chi_{BS}N\varphi_S + \xi(\vec{r}) \tag{13}$$

$$w_C(\vec{r}) = \chi_{AC}N\varphi_A + \chi_{BC}N\varphi_B + \chi_{CS}N\varphi_S + \xi(\vec{r}) \tag{14}$$

$$w_S(\vec{r}) = \chi_{AS}N\varphi_A + \chi_{BS}N\varphi_B + \chi_{CS}N\varphi_C + \xi(\vec{r}) \tag{15}$$

$$\varphi_A(\vec{r}) + \varphi_B(\vec{r}) + \varphi_C(\vec{r}) + \varphi_S(\vec{r}) = 1 \tag{16}$$

We solve the self-consistent field Equations (8–16) in real space, and it is assumed that the equilibrium is reached when the relative

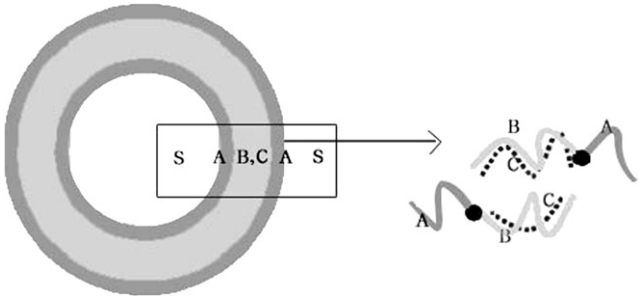

Fig. 3. Schematic illustration of a bilayer vesicle consisting of copolymer *AB*, homopolymer *C*, and solvent *S*.

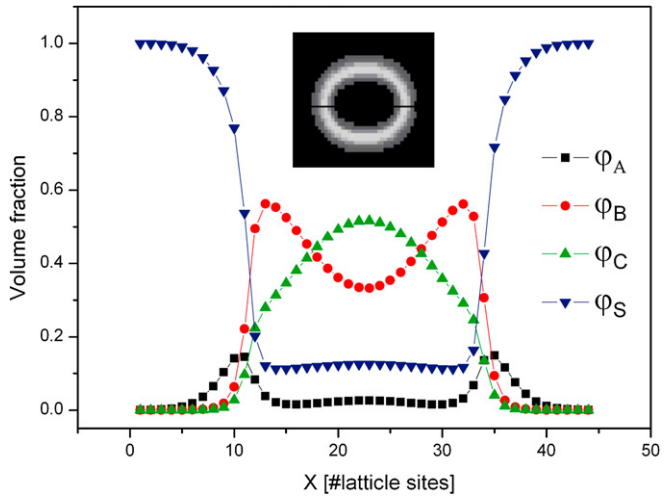

Fig. 4. (Color online) Density distributions of each constituent along the intercepting line through the center of a micelle in the amphiphilic system corresponding to (b) in Fig. 1 except $\chi_{BS}N = \chi_{CS}N = 40.0$. (For interpretation of the references to color in this figure legend, the reader is referred to the web version of this article.)

change in the free energy between two consecutive iteration steps is smaller than 10^{-6} (namely $\Delta F < 10^{-6}$). We use random initial condition in our iterative algorithm to generate a large set of solutions to the mean-field equations over a wide range of phase space. We take the equilibrium phase to be the structure which has the lowest free energy. All the simulations are repeated by using different random numbers to guarantee that the observed structures are not artifacts. In the calculations, the sizes of the computational domain are $L_x = L_z = 20R_g$ with R_g the radius of gyration of the copolymer chain, the grid size are $\Delta_x = \Delta_z = 0.05R_g$. Periodic boundary is used along x-direction and z-direction, and the length scale is in the unit of R_g.

3. Results and discussion

We employ SCFT theory to examine the phase behaviors and the vesicle formation in a solution of linear *AB* diblock copolymers and linear *C* homopolymers in *S* solvent. We consider a dilute solution with 10% of the solute, namely $\overline{\varphi}_{AB} + \overline{\varphi}_C = 0.1$, $\overline{\varphi}_S = 0.9$. The diblock copolymer chain consists of the hydrophilic segment *A* and the hydrophobic segment *B*. Furthermore, homopolymer *C* is assumed to be completely miscible with the block *B* such that $\chi_{BC} = 0.0$. The fraction of *A*-monomer in a copolymer chain is fixed as $f = 0.25$ and the chain length of the diblock copolymer is set to $N = 24$ in this paper, and the chain length of homopolymer *C* is set to $N_C = 12$ in this paper except in Fig. 9.

First the microstructures assembled in the dilute block copolymer/homopolymer solution are studied by varying the concentration radio of copolymer *AB* and homopolymer *C*. The microstructures and the density distributions of block *A* when the concentration ratio is varied between $\overline{\varphi}_{AB}/\overline{\varphi}_C \in [0.04/0.06, 0.09/0.01]$ at fixed polymer volume fraction $\overline{\varphi}_{AB} + \overline{\varphi}_C = 0.1$ are shown in Fig. 1. As can be seen from (a) and (b) in Fig. 1, at $\overline{\varphi}_{AB} = 0.04, 0.05$, only vesicles emerge from the solution. As the volume fraction of $\overline{\varphi}_{AB}$ is further increased, mixed morphologies consisting of rod-like, circle-like micelles as well as vesicles dominate the phase behaviors of the mixture. At $\overline{\varphi}_{AB} = 0.09$ corresponding to (f) in Fig. 1, the micellar microstructure dominates over the vesicular microstructure. The density distributions of various constituents in the mixture across a line cutting through the center of a vesicle are shown in Fig. 2. From Fig. 2, it can be seen that between the inner and the outer interfaces of the bilayer-structured vesicle, the hydrophobic block *B* is enriched substantially. Whereas the enrichment of homopolymer *C* inside the membrane is only moderate and its distribution inside the membrane is more or less uniform. Inside the membrane the depletion of the hydrophilic block *A* is not very strong. There is still some solvent present inside the membrane of the vesicle presumably due to not strong enough repulsive interactions between *B*, *C* with the solvent molecules. From (a–f) in Fig. 1, the volume fraction of homopolymer *C* which contributes to the formation of the

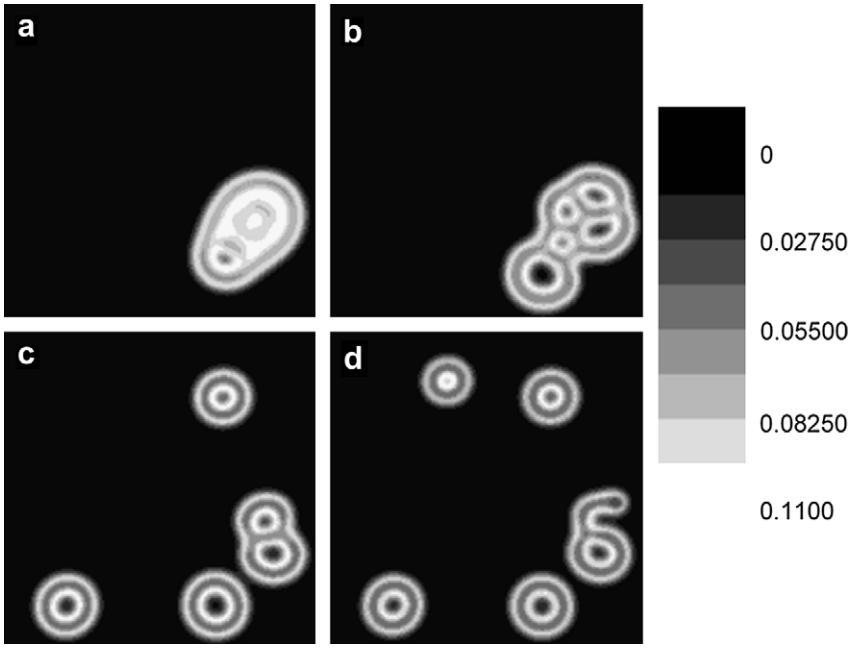

Fig. 5. Density distributions of diblock *A* and *B*, homopolymers *C*, and solvent *S*. The interaction parameters of the system are $\chi_{AS}N = 0.5$, $\chi_{BS}N = 30.0$, $\chi_{CS}N = 20.0$, $\chi_{BC}N = 0.0$, $\chi_{AB}N = 9.0$, $\chi_{AC}N = 2.0$. From (a–d), the copolymer concentration $\overline{\varphi}_{AB}$ is increasing with: $\overline{\varphi}_{AB} = 0.035$ (a), $\overline{\varphi}_{AB} = 0.039$ (b), $\overline{\varphi}_{AB} = 0.05$ (c), $\overline{\varphi}_{AB} = 0.052$ (d).

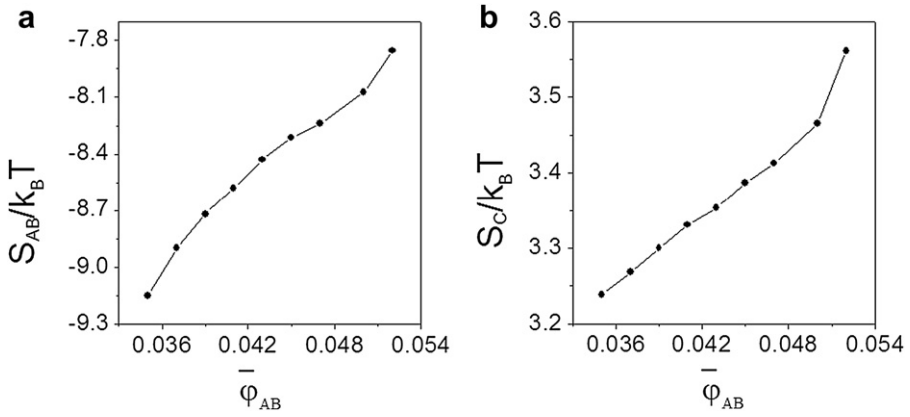

Fig. 6. (a) Entropy of a single block copolymer chain S_{AB}/k_BT, (b) entropy of a single homopolymer chain S_C/k_BT as a function of the diblock volume fraction $\overline{\varphi}_{AB}$.

membrane of the vesicle is decreasing, resulting in the decrease of the packing parameter of the amphiphilic system [1]. Therefore, from (a–f) in Fig. 1, micellar structures are more favored. With the decrease of the volume fraction of homopolymer *C*, the thickness of the membrane of the bilayer vesicle also decreases. The thickness of the membrane of the bilayer vesicle is estimated to be about $0.5R_g$ (about 10 grid sizes) of the diblock copolymer chain from the density profiles shown in Fig. 2. This thickness corresponds to about 0.6 of the radius of gyration of a chain with the same chain length as the hydrophobic block *B*. Moreover, the density distribution of block *B* shows a single peak inside the membrane. Thus, the partial interdigitation of the block *B* chains anchored on the outer and inner interfaces should be expected as shown in the schematic illustration of the structure of the bilayer vesicle displayed in Fig. 3.

The vesicles formed corresponding to the systems shown in Fig. 1 contain appreciable amount of the solvent *S* (volume fraction ~0.3), and it would be interesting to see if the solvent *S* inside the membrane of the vesicles can be depleted if the repulsive interactions between the solvent *S* and the hydrophobic block *B* and homopolymer *C* are further increased. In the simulations, the interaction parameters $\chi_{BS}N$ and $\chi_{CS}N$ are both increased from 30.0 to 20.0–40.0. However, it is found that only micelles appear and no bilayer vesicles emerge. The density distributions of various constituents in the system along the intercepting line through the center of a typical circle-like micelle are displayed in Fig. 4. It can be easily seen from Fig. 4 that the *AB* diblock copolymer is distributed along the circumference of the micelle. Inside the micelle, the concentration of the solvent *S* is much lower than that in Fig. 1, and the concentration of the homopolymer *C* reaches a maximum at the center of the circle-like micelle, indicating the enrichment of *C* at the center of the micelle.

The morphology of compound vesicles which has been observed in experiments and previous SCFT simulations [30,40], have been explored in our simulations. By decreasing the repulsive interaction between block *A* and homopolymer *C* while keeping the rest interaction parameters unaltered, the formation of compound vesicle is observed in the simulations as shown in Fig. 5. At relatively low concentration of block *AB*, $\overline{\varphi}_{AB} = 0.035$, due to the homogenizing effect of the homopolymer *C* with both *A* and *B* and its relatively high concentration, the degree of the phase-separation is not strong as shown in (a) of Fig. 5. As the concentration of block *AB* is slightly increased to $\overline{\varphi}_{AB} = 0.039$, the compound vesicle is clearly seen in (b) of Fig. 5. As the volume fraction of block copolymer *AB* further increases, the compound vesicle is replaced by unilamellar vesicles. At higher *AB* concentration, the entropic effect of *AB* diblock copolymer becomes dominant, so the unilamellar vesicle morphology is more favored than the compound vesicle morphology entropically. In Fig. 6, the entropic parts of the free energies of a single *AB* diblock copolymer and *C* homopolymer chain are displayed for different morphologies shown in Fig. 5. The

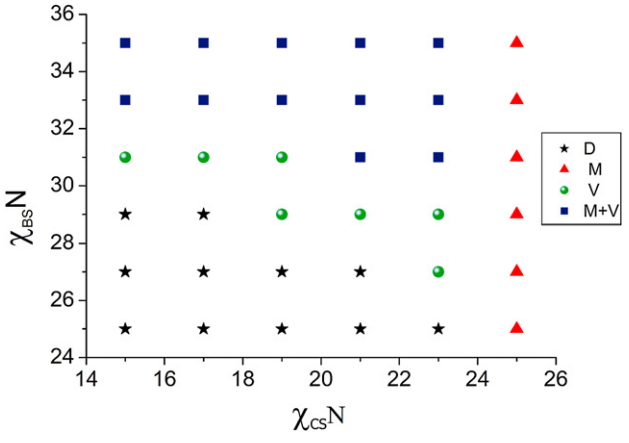

Fig. 7. (Color online) Phase structures are plotted as function the Flory–Huggins interaction parameters $\chi_{BS}N$ and $\chi_{CS}N$. The interaction parameters of the system are $\chi_{AS}N = 0.5$, $\chi_{BC}N = 0.0$, $\chi_{AB}N = \chi_{AC}N = 9.0$, $\overline{\varphi}_{AB} = 0.05$. (For interpretation of the references to color in this figure legend, the reader is referred to the web version of this article.)

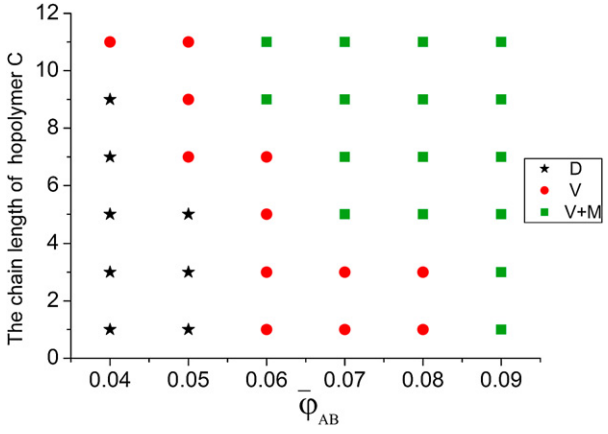

Fig. 8. (Color online) Phase diagram of an amphiphilic diblock copolymer/homopolymer solution plotted as functions of the chain length of homopolymer *C* and diblock volume fraction $\overline{\varphi}_{AB}$. The interaction parameters of the system are $\chi_{AS}N = 0.5$, $\chi_{BS}N = 30.0$, $\chi_{CS}N = 20.0$, $\chi_{BC}N = 0.0$, $\chi_{AB}N = \chi_{AC}N = 9.0$. (For interpretation of the references to color in this figure legend, the reader is referred to the web version of this article.)

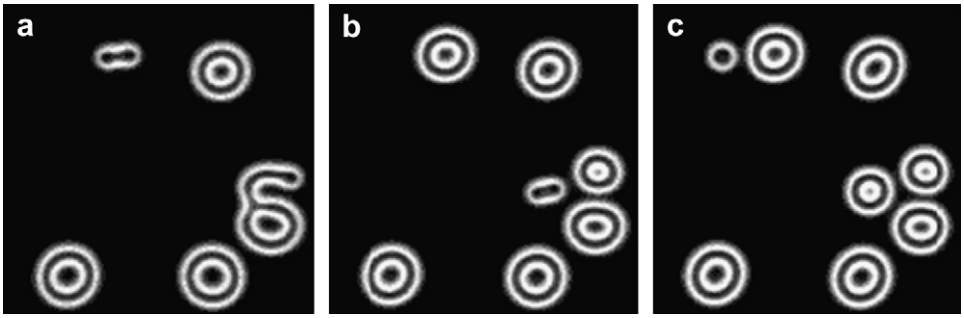

Fig. 9. Density distributions of diblock *A* and *B* in the amphiphilic system, containing small hydrophobic molecule *C*. In the system, the interaction parameters are $\chi_{AB}N = 9.0$, $\chi_{AS}N = 0.5$, $\chi_{BS}N = 30.0$, $\chi_{CS}N = 20.0$, $\chi_{BC}N = 0$, $\chi_{AC}N = 9.0$. The copolymer concentration $\overline{\varphi}_{AB}$ is increasing from (a–c) with $\overline{\varphi}_{AB} = 0.07$ (a), $\overline{\varphi}_{AB} = 0.08$ (b) and $\overline{\varphi}_{AB} = 0.09$ (c).

entropies of a single block copolymer chain and a single homopolymer chain are obtained from the following two expressions:

$$S_{AB}/k_B = \ln\left(\frac{Q_{AB}}{\overline{\varphi}_{AB}V}\right) + \frac{1}{\overline{\varphi}_{AB}V}\int d\vec{r}\,(w_A(\vec{r})\varphi_A(\vec{r}) + w_B(\vec{r})\varphi_B(\vec{r})) \quad (17)$$

$$S_C/k_B = \ln\left(\frac{Q_C}{\overline{\varphi}_C V}\right) + \frac{N_C}{N\overline{\varphi}_C V}\int d\vec{r}\, w_C(\vec{r})\varphi_C(\vec{r}) \quad (18)$$

Fig. 6 clearly shows that the entropies of a single block copolymer and homopolymer chain increase with the increase of the volume fraction $\overline{\varphi}_{AB}$.

We have further investigated the effect of the interactions among the polymer chains and the solvent molecules on the aggregation behavior of the diblock copolymer/homopolymer solution. Because there are quite a few interaction parameters involved in this system, e.g., $\chi_{AB}N$, $\chi_{AC}N$, $\chi_{AS}N$, etc., for simplicity, we limit us to the case that $\chi_{BS}N$, $\chi_{BS}N$ are systematically varied while keeping all other interaction parameters and chain lengths the same as in Fig. 1; also, the volume fraction of $\overline{\varphi}_{AB}$ is fixed at 0.05. The aggregate morphological stability regions are illustrated in Fig. 7. Four characteristic zones can be clearly identified in the phase diagram: disorder state (D), micelles (M), vesicles (V), and mixture of micelles and vesicles (M + V). It can be clearly seen from Fig. 7 that the micelle morphology emerges exclusively when $\chi_{CS}N \geq 25$.

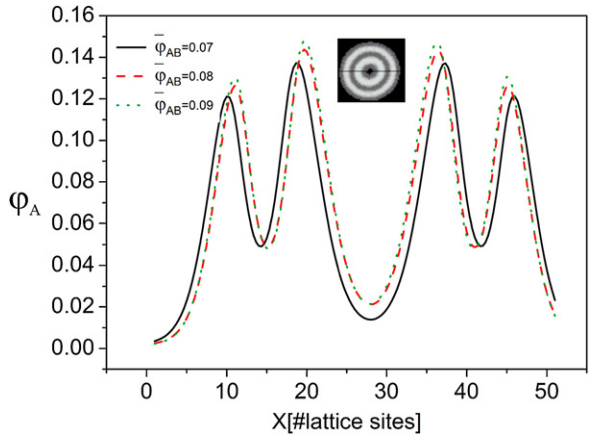

Fig. 10. (Color online) Density distributions of block *A* along the intercepting line through the center of the vesicle at different averaged volume fractions of diblock copolymer $\overline{\varphi}_{AB}$. In the figure, the two shallower valleys correspond to the membranes between the inner and outer interfaces. (For interpretation of the references to color in this figure legend, the reader is referred to the web version of this article.)

The chain length of homopolymer *C* can strongly influence the morphologies of the amphiphilic system. Here the morphology stability regions are constructed by varying the chain length of homopolymer *C* and the volume fraction $\overline{\varphi}_{AB}$ while keeping all Flory–Huggins interaction parameters the same as those in Fig. 1 and are shown in Fig. 8. Three characteristic zones can be clearly identified in the phase diagram: disorder state (D), vesicles (V), and mixture of vesicles and micelles (V + M). It can clearly seen that, for relatively short homopolymer *C* chain length and low volume fraction $\overline{\varphi}_{AB}$, disordered phase is favored. For longer chain length and higher volume fraction, the mixed morphology of vesicles and micelles becomes dominant.

The effect of the degree of polymerization of the homopolymer *C* on the vesicle formation of the binary amphiphilic block copolymer/homopolymer system is interesting, particularly for the case that the homopolymer *C* becomes a monomer, namely a small solvent molecule immiscible with the solvent *S*. As such, the system turns into one with a single-component block copolymer in a binary immiscible solvent mixture, which has relevance to the double emulsions in the form of either water-in-oil-in-water or oil-in-water-in-oil. Due to their compartmentalized internal structure, double emulsions can provide advantages over simple oil-in-water emulsions for encapsulation of both polar and non-polar cargos and the improved control of drug release. The preparation of the double emulsions typically requires the use of mixtures of surfactants for the stability. Very recently, Hanson et al. reported the preparation of water-in-oil-in-water double emulsions using a single-component synthetic amphiphilic diblock copolypeptide [45]. The diblock copolypeptide consists of hydrophilic highly charged poly(L-lysine) block and the hydrophobic flexible poly(racemic-leucine) block. The hydrogen bonding interaction among the rac-leucine segments in the oil phase is the key to the stabilization of the double emulsions, preventing the internal droplet coalescence. Because in our simulations, the block copolymer is coarse-grained and the molecular details are smeared out, it is unlikely that our generic model can reproduce the Hanson's experimental results. Nevertheless, the vesicle formation in single-component diblock copolymer in binary immiscible solvent mixture is interesting and has not been studied theoretically, thus we carried out this study by reducing the homopolymer *C* to a monomer-type solvent molecule.

In the simulations, the interaction parameters are kept the same as those in Fig. 1 with the total volume fraction of *AB* and *C* fixed at 0.1, and the chain length of homopolymer is reduced to one, thus rendering *C* a small solvent molecule. As can be seen from Fig. 9, as the volume fraction of *AB* diblock copolymer further increases, the bilayer vesicle structure becomes dominant. Unlike the morphologies in the case of *C* being a polymer chain as shown in Fig. 1 where the micelle structures are dominant over the vesicle structure at

high *AB* volume fraction, the vesicle morphology is dominant when the component *C* is a small solvent molecule as shown in Fig. 9. This difference in the morphologies is due to the different roles played by the component *C* when it is a polymer chain or a small solvent molecule. Being a small solvent molecule, the component *C* is irrelevant to the packing parameter of the single component block copolymer amphiphilic system, which is determined by three factors related to the block copolymer chain: the chain volume, the chain length of the hydrophobic block and the so-called optimal head group area related to the size of the hydrophilic block. Thus as the volume fraction of *AB* block copolymer increases, the packing parameter is unaltered, so no morphological change is observed. In Fig. 10, the density distribution of block *A* along the intercepting line through the center of a vesicle at different averaged volume fractions of the diblock copolymer *AB* is displayed, from which the thickness of the membrane of the vesicle can inferred. It can be seen from Fig. 10 that the thickness of the membrane remains unchanged as the volume fraction of solvent molecule *C* decreases, implying that the packing parameter indeed does not depend on the small solvent *C*.

4. Conclusion

We have studied the morphologies and the vesicle formation in a binary amphiphilic diblock copolymer *AB*/homopolymer *C* in a dilute solution by using real space self-consistent field theory (SCFT) in 2D. The morphologies and the vesicle formation in this system were controlled by fine tuning the competing interactions in the amphiphilic system, namely the chain stretching in the core, the interfacial tension and the repulsion among corona chains. In the study, special attention was paid to the role played by the homopolymer *C*. The tuning of the competing interactions in the system was performed by adjusting the volume fraction, interaction parameters and the degree of polymerization of the homopolymer *C*. In the simulations, it was found that as the averaged volume fraction of homopolymer *C* decreased while keeping the total averaged volume fraction of block copolymer *AB* and homopolymer *C* unchanged, there was a morphological transition from the bilayer vesicles to rod-like/circle-like micelles. This transition was induced by the decreasing of the packing parameter of the amphiphilic system due to the decrease of the averaged volume fraction of the homopolymer. Inside the membranes of the bilayer vesicles, there was appreciable amount of the solvent and the hydrophobic block *B* was partially interdigitated.

To deplete the solvent from the membrane, the repulsive interactions between the solvent with the hydrophobic block *B* and the homopolymer *C* were further increased. However, this led to the disappearance of the vesicular morphology and the emergence of the circle-like micelles inside which the block *B* and homopolymer were enriched and the solvent was depleted. The compound vesicle structure was also observed in the simulations. With the further increase of the averaged volume fraction of block copolymer *AB*, the compound vesicle structure became less favored entropically than the unilamellar vesicle structure, thus the unilamellar vesicle structure was the dominant structure in the system.

The effect of the degree of polymerization of the homopolymer *C* on the vesicle formation of the amphiphilic system was examined. By reducing the degree of polymerization of the homopolymer *C* to unity, the component *C* became a small solvent molecule immiscible with the bulk solvent. It was found that the small solvent *C* exerted no influence on the morphological stability of the vesicles, and the packing parameter of the system did not dependent on the averaged volume fraction of the small solvent *C*. It is anticipated that the present study will stimulate future researches on the formation of double emulsions, i.e., water-in-oil-in-water or oil-in-water-in-oil, in a single-component amphiphilic block copolymer in a binary solvent mixture.

Acknowledgments

We thank Dr. Chunlai Ren for helpful discussions. This work is supported by the National Natural Science Foundation of China under Grant No.10774079, Natural Science Foundation of Ningbo Grant No.2009 A610056 and K. C. Wong Magna Fund in Ningbo University.

References

[1] Israelachvili J. Intermolecular and surface forces. New York: Academic Press; 1991.
[2] Luo LB, Eisenberg A. J Am Chem Soc 2001;123:1012–3; Yu K, Eisenberg A. Macromolecules ;31:3509–18; Burke S, Shen HW, Eisenberg A. Macromol Symp ;175:273–83.
[3] Zhang LF, Eisenberg A. Macromolecules 1996;29:8805–15.
[4] Discher DE, Eisenberg A. Science 2002;297:967–73.
[5] Gao ZS, Eisenberg A. Macromolecules 1993;26:7353–60.
[6] Zhang L, Eisenberg A. Science 1995;268:1728–31.
[7] Van Hestm JCM, Delnoye DAP, Baars MWPL, Van Genderen MHP, Meijer EW. Science 1995;268:1592–5.
[8] Tu YF, Wan X, Zhang D, Zhou QF, Wu C. J Am Chem Soc 2000;122:10201–5.
[9] Li ZB, Kesselman E, Talmon Y, Hillmyer MA, Lodge TP. Science 2004;306:98–101.
[10] Yan DY, Zhou YF, Hou J. Science 2004;303:65–7.
[11] Cheng C-X, Huang Y, Tang R-P, Chen E-Q, Xi F. Macromolecules 2005;38:3044–7.
[12] Massey JA, Temple K, Cao L, Rharbi Y, Raez J, Winnik MA, et al. J Am Chem Soc 2000;122:11577–84.
[13] Jain S, Bates FS. Macromolecules 2004;37:1511–23; Pochan DJ, Chen Z, Cui H, Hales K, Qi K, Wooley KL. Science ;306:94–7; Gohy J-F, Willet N, Varshney S, Zhang JX, Jérôme R. Angew Chem Int Ed ;40:3214–6.
[14] Schrage S, Sigel R, Schlaad H. Macromolecules 2003;36:1417–20; Weaver JVM, Armes SP, Liu S. Macromolecules ;36:9994–8.
[15] Grubbs RB. J Polym Sci Part A Polym Chem 2005;43:4323–36;
Hu J, Liu G. Macromolecules 2005;38:8058–65;
Yan X, Liu G, Hu J, Willson CG. Macromolecules 2006;39:1906–12.
[16] Miao Bing, Yan Dadong, Wickham Robert A, Shi An-Chang. Polymer 2007;48:4278–87.
[17] Nojima Shuichi, Ito Keisuke, Ikeda Hiroshi. Polymer 2007;48. 3607–3611.
[18] Li Xue, Peng Juan, Wen Yan, Kim Dong Ha, Knoll Wolfgang. Polymer 2007;48:2434–43.
[19] He XH, Schmid F. Macromolecules 2006;39:2654–62.
[20] He XH, Schmid F. Phys Rev Lett 2008;100:137802 (1–4).
[21] Lipowsky R. Nature 1991;349:475–81.
[22] Julicher F, Lipowsky R. Phys Rev Lett 1993;70:2964–7.
[23] Umeda T, Nakajima H, Hotani H. J Phys Soc Jpn 1998;67:682–8.
[24] Bernardes AT. J Phys II 1996;6:169–74.
[25] Bernardes AT. Langmuir 1996;12:5763–7.
[26] Noguchi H, Takasu M. Phys Rev E 2001;64:041913–9.
[27] Noguchi H, Takasu M. J Chem Phys 2001;115:9547–51.
[28] Sevink GJA, Zvelindovsky AV. Macromolecules 2005;38:7502–13.
[29] Yamamoto S, Maruyama Y, Hyodo S-A. J Chem Phys 2002;116:5842–9.
[30] He XH, Liang HJ, Huang L, Pan CY. J Phys Chem B 2004;108:1731–5.
[31] Jiang Y, Chen T, Ye FW, Liang HJ, Shi A-C. Macromolecules 2005;38:6710–7.
[32] Wang R, Tang P, Qiu F, Yang YL. J Phys Chem B 2005;109:17120–7.
[33] Monzen M, Kawakatsu T, Doi M, Hasegawa R. Comput Theor Polym Sci 2000;10:275–80.
[34] Tsuchida E, Abe K. Adv Polym Sci 1982;45:1–119.
[35] Jiang M, Li M, Xiang M, Zhou H. Adv Polym Sci 1999;146:121–96.
[36] Oyama HT, Tang WT, Frank CW. Macromolecules 1987;20:474–80.
[37] Hemker DJ, Garza V, Frank CW. Macromolecules 1990;23:4411–8.
[38] Khutoryanskiy VV, Dubolazov AV, Nurkeeva ZS, Mun GA. Langmuir 2004;20:3785–90.
[39] Lutkenhaus JL, Hrabak KD, McEnnis K, Hammond PT. J Am Chem Soc 2005;127:17228–34.
[40] Gao WP, Bai Y, Chen EQ, Li ZC, Han BY, Yang WT, et al. Macromolecules 2006;39:4894–8.
[41] Muler Christian, Radano Christopher P, Smith Paul, Stingelin-Stutzmann Natalie. Polymer 2008;49:3973–8.
[42] Jiang Zhiping, Zhu Zhengsu, Liu Chengjie, Hu Yong, Wu Wei, Jiang Xiqun. Polymer 2008;49:5513–9.
[43] Tsuchiya Kousuke, Shimomura Takeshi, Ogino Kenji. Polymer 2009;50:95–101.
[44] Daniel Gromadzki, Jan Lokaj, Miroslav Slouf, Petr Stpanek. Polymer 2009;50:2451–9.
[45] Hanson JA, Chang CB, Graves SM, Li ZB, Mason TG, Deming TJ. Nature 2008;455:85–9.